Published in final edited form as:
Neuroimage. 2007 February 15; 34(4): 1342–1351.

IMAGING SIGNAL TRANSDUCTION *VIA* ARACHIDONIC ACID IN THE HUMAN BRAIN DURING VISUAL STIMULATION, BY MEANS OF POSITRON EMISSION TOMOGRAPHY

Giuseppe Esposito, M.D.[1,4], **Giampiero Giovacchini, M.D.**[2,6], **Margaret Der**[2], **Jeih-San Liow, Ph.D.**[1], **Abesh K. Bhattacharjee, M.D., Ph.D.**[1], **Kaizong Ma, M.S.**[1], **Peter Herscovitch, M.D.**[2], **Michael Channing, Ph.D.**[2], **William C. Eckelman, Ph.D.**[2,7], **Mark Hallett, M.D.**[3], **Richard E. Carson, Ph.D.**[2,5], and **Stanley I. Rapoport, M.D.**[1,*]

1 *Brain Physiology and Metabolism Section, National Institute on Aging, National Institutes of Health, Bethesda, MD*

2 *PET Department, Warren Magnusson Clinical Center, National Institutes of Health, Bethesda, MD*

3 *Human Motor Control Section, Medical Neurology Branch, National Institute of Neurological Disease and Stroke; National Institutes of Health, Bethesda, MD*

5 *Department of Diagnostic Radiology and Biomedical Engineering, Yale University, New Haven, CT;*

6 *Department of Radiology, University of Pisa, Pisa, Italy*

7 *Molecular Tracer, LLC, Snow Point Drive, Bethesda MD*

Abstract

Background—Arachidonic acid (AA, 20:4n-6), an important second messenger, is released from membrane phospholipid following receptor mediated activation of phospholipase A_2 (PLA_2). This signaling process can be imaged in brain as a regional brain AA incorporation coefficient K*.

Hypothesis— K* will be increased in brain visual areas of subjects submitted to visual stimulation.

Subjects and methods— Regional values of K* were measured with positron emission tomography (PET), following the intravenous injection of [1-^{11}C]AA, in 16 healthy volunteers subjected to visual stimulation at flash frequencies 2.9 Hz (8 subjects) or 7.8 Hz (8 subjects), compared with the dark (0 Hz) condition. Regional cerebral blood flow (rCBF) was measured with intravenous [^{15}O]water under comparable conditions.

Results— During flash stimulation at 2.9 Hz or 7.8 Hz vs. 0 Hz, K* was increased significantly by 2.3–8.9% in Brodmann areas 17, 18 and 19, and in additional frontal, parietal and temporal cortical regions. rCBF was increased significantly by 3.1% – 22%, often in comparable regions. Increments at 7.8 Hz often exceeded those at 2.9 Hz for both K* and rCBF. Decrements in both parameters also were produced, particularly in frontal brain regions.

Conclusions— AA plays a role in signaling processes provoked by visual stimulation, since visual stimulation at flash frequencies of 2.9 and 7.8 Hz compared to 0 Hz modifies both K* for AA and rCBF in visual and related areas of the human brain. The two-stimulus condition paradigm of this

*Corresponding Author: Brain Physiology and Metabolism Section, Bldg. 9, Rm. 1S128, National Institute on Aging, National Institutes of Health, 9 Memorial Drive, Bethesda, MD 20892, Tel: 301 496 1765, Fax: 301 402 0074, E-mail: sir@helix.nih.gov
[4]Present addresses: Department of Nuclear Medicine, Washington Hospital Center, Washington, DC;

study might be used with PET to image effects of other functional activations and of drugs on brain signaling *via* AA.

Keywords

positron emission tomography; brain; human; arachidonic acid; stimulation; phospholipase A_2; signal; transduction; blood flow; visual; flash; sensory

Introduction

In the field of *in vivo* human neuroimaging, no reliable method currently exists to examine regional brain signal transduction in response to pharmacological or functional activation. Yet post-mortem and *in vivo* measurements of neuroreceptor and neurotransporter densities suggest that disturbed brain signal transduction might contribute to changes in behavior involving neurotransmission in a number of human diseases, including bipolar disorder, depression, Parkinson disease, schizophrenia and attention deficit hyperactivity disorder (Cooper et al. 2003;Rakshi et al. 2002;Rapoport and Bosetti 2002;Solanto 2002).

In a series of *in vivo* studies in rodents, we have developed such a method to image brain signal transduction that involves the second messenger, arachidonic acid (AA, 20:4n-6), using quantitative autoradiography following the intravenous injection of radiolabeled AA. This method measures the consequences of AA release from membrane phospholipids by the neuroreceptor-mediated activation of phospholipase A_2 (PLA_2), in terms of a regional brain incorporation coefficient K* (brain radioactivity/integrated plasma radioactivity). We reported regional increments in K* following visual activation (Wakabayashi et al. 1995) or administration to rats of agonists to cholinergic muscarinic $M_{1,3,5}$ receptors (Basselin et al. 2006b), dopaminergic D_2-like receptors (Bhattacharjee et al. 2005), serotonergic 5-$HT_{2A/2C}$ receptors (Qu et al. 2003), N-methyl-D-aspartate (NMDA) receptors (Basselin et al. 2006a), and nicotinic receptors (Nguyen et al. 2006), all of which can be coupled to activation of Ca^{2+}-dependent AA-selective cytosolic $cPLA_2$ to release AA (Bayon et al. 1997;Clark et al. 1995;Stout et al. 2002;Vial and Piomelli 1995;Weichel et al. 1999). The increments following drug occurred at regions with high densities of the targeted neuroreceptor, could be blocked by pre-treatment with the receptor antagonist or a PLA_2 inhibitor (Grange et al. 1998), were shown to reflect incorporation of unesterified AA from plasma into synaptic membrane phospholipid (Jones et al. 1996), and were unaffected by changes in regional cerebral blood flow (rCBF) (Chang et al. 1997;DeGeorge et al. 1991;Robinson et al. 1992).

We also have extended our fatty acid method to image K* for AA using positron emission tomography (PET) in human subjects at rest, following the intravenous injection of [1-^{11}C] AA (Chang et al. 1997;Channing and Simpson 1993;Giovacchini et al. 2002;Giovacchini et al. 2004). In the present study, we further extend our PET method, when using a two-condition stimulation paradigm, to image the effects of visual flash stimulation on K* for AA in relation to effects on rCBF. Briefly, in the same PET session, we exposed healthy volunteers to light flashes at frequencies of 0 Hz (dark condition) and of either 2.9 Hz or 7.8 Hz, and measured K* for AA as well as rCBF with [^{15}O]water in both conditions.

We chose visual flash stimulation for this study because we had used such stimulation previously to show that rCBF changed in wide regions of the brain in healthy and Alzheimer disease subjects exposed to flash frequencies between 0 Hz and 14 Hz (Mentis et al. 1997;Mentis et al. 1998;Mentis et al. 1996), thus giving us a published frame of reference for expected rCBF and K* changes. In healthy subjects, we and others (Fox et al. 1984) reported that rCBF in the primary (striate) visual cortex increased between flash stimulation frequencies of 0 and 7–8 Hz, then declined at higher frequencies. Continually increasing, biphasic or

decreasing frequency-dependent changes in rCBF occurred in other brain areas within the two visual association streams, as well as in areas outside of these streams (Ungerleider and Mishkin 1982).

Functional activity in brain visual areas can involve neurotransmission *via* a number of neuroreceptor subtypes, particularly glutamatergic receptors, that are coupled to $cPLA_2$ activation and AA release (see above) (Edagawa et al. 2000;Yashiro et al. 2005;Zhao et al. 2001). We hypothesized that changes in K* at 3.9 and 7.8 Hz compared with 0 Hz would occur largely in the regions in which rCBF was altered, reflecting such neurotransmitter-mediated $cPLA_2$ activation. As noted above, K* itself is not influenced by changes in rCBF, but measures only the AA released *and* lost by metabolism during activation (Basselin et al. 2006b;Chang et al. 1997;DeGeorge et al. 1991;Robinson et al. 1992). Part of our work has been presented in abstract form (Esposito et al. 2003).

Material and Methods

Subjects

Sixteen healthy volunteers (age range 22–39 years; 11 M, 5 F) were studied under Protocol No. 00-N-0057. The protocol was approved by the Institutional Review Board of the National Institute on Neurological Diseases and Stroke, and by the NIH Radioactive Drug Research and Radiation Safety Committees. Each subject gave informed written consent after the purpose and risks of the study were explained. Exclusion criteria were a past or current medical condition that could interfere with brain function, such as alcoholism, psychiatric illness, head trauma, exposure to central nervous system toxin, hypertension or other cardiovascular disorders, diabetes, malignancy and psychopharmacological treatment. Subjects were off medication for 2 weeks, off aspirin for 2 days, and off caffeine and alcohol for at least 12 hours prior to their PET session. Magnetic resonance imaging (MRI) of the head was performed to exclude brain pathology and to analyze the functional PET scans.

Radiochemistry

[1-^{11}C]AA was produced in one synthesis, as previously described (Chang et al. 1997;Channing and Simpson 1993;Giovacchini et al. 2002). The volume of synthesized tracer was divided at a ratio of 1:8, then reconstituted into two equal volumes for the first and second [1-^{11}C]AA injections, respectively. This ratio provided roughly equivalent doses for the two scans, given the 20.4-minute half-life of ^{11}C. On average, a single [1-^{11}C]AA synthesis yielded 10730 ± 107.3 (S.D.) mCi, allowing 554 ± 116 MBq (14.9 ± 3.1 mCi) of [1-^{11}C]AA for the first scan, and 507 ± 100 MBq (13.7 ± 2.7 mCi) for the second.

Positron emission tomography

A catheter was inserted into a radial artery for blood withdrawal, and a needle was inserted into a forearm vein for radiotracer injection. PET scans were obtained with a General Electric Advance Tomograph (Waukesha, WI), and a transmission scan was acquired to correct for attenuation. Then, each subject received in fixed order four [^{15}O]water scans to measure rCBF, and two [1-^{11}C]AA scans to measure K* for AA.

[^{15}O]water scans

The [^{15}O]water scans were performed every 15 min. For each scan, a bolus of 370 MBq (10 mCi) [^{15}O]water was injected intravenously, and blood was withdrawn continuously through the radial artery catheter, using an automated withdrawal and counting system. From initial 1-min scans, rCBF was calculated by an autoradiographic method (Herscovitch et al. 1983).

[1-^{11}C]AA scans

The first [1-^{11}C]AA scan was started 15 min after the last [^{15}O]water injection, the second 60 min after the first [1-^{11}C]AA injection. After each injection, serial dynamic 3-D scans (30 sec to 5 min) were acquired during 1 hour. For each scan, [1-^{11}C]AA was infused intravenously for 3 min at a constant rate (Harvard Infusion Pump, South Natick, MA, USA), and the input function was measured as previously described (Giovacchini et al. 2002;Giovacchini et al. 2004).

Visual stimulation paradigm

A subject was scanned during each of two visual stimulation conditions in the same PET session, a dark condition (0 Hz) or when exposed to flashing lights at a frequency of 2.9 Hz or 7.8 Hz. Stimulation consisted of red flashing lights delivered by goggles (Model S10Vs B, Grass Instruments, Quincy, MA), with eyepieces containing 30 monochromatic red light-emitting diodes (LED) in a 6 × 5 rectilinear grid with a mean peak of 655 nm. The grids were not centered over the fovea but formed an overlapping pattern on the visual fields. The flashes were delivered as 5-ms square wave pulses, alternately to each eye (Mentis et al. 1997), and frequency was defined as the number of flashes presented to one eye per second. Each LED had a luminous intensity of 3.6 millicandela. As flash duration was 5 ms, increasing flash frequency decreased the flash interval and increased luminosity.

In one session, eight subjects were stimulated at 0 Hz (dark) and 2.9 Hz, eight at 0 Hz and 7.8 Hz. A subject wore the goggles during the entire PET session. He was instructed to keep his eyes closed under the dark condition (0 Hz), but to keep them open during stimulation at 2.9 or 7.8 Hz. The scan order was randomized across subjects according to two different sequences:

1. Dark (0 Hz) rCBF → stimulation rCBF → stimulation rCBF → dark rCBF → dark K* for AA → stimulation K* for AA

   or

2. Stimulation rCBF → dark (0 Hz) rCBF → dark rCBF → stimulation rCBF → stimulation K* for AA → dark K* for AA

During the dark (0 Hz) condition, the steps to measure rCBF were as follows: 10 min before [^{15}O]water injection, dim lights in PET room; 5 min before injection, turn off lights in PET room (staff will use side-shielded flashlights); inject [^{15}O]water intravenously as bolus, and remove arterial blood samples as scheduled and scan for 1 min; wait 15 min for next injection. For the K* scan, infuse [1-^{11}C]AA intravenously for 3 min, maintaining 0 Hz (dark) condition; remove arterial blood samples and scan for 1 hour.

During the 2.9 Hz or 7.8 Hz stimulation condition, for the rCBF scan, follow the procedure above to 15 min except stop stimulation after 2 min and go to dark condition for the following 13 min. For the K* scan, at 15 min after injecting [^{15}O]water, start stimulation at 2.9 or 7.8 Hz; 15 sec later, infuse [1-^{11}C]AA for 3 min intravenously, remove arterial blood samples and scan for 1 hour. At 10 min after beginning [1-^{11}C]AA infusion, change to dark (0 Hz) condition for 1 min to minimize possible discomfort from continuously applied flashing lights; repeat 4 min of flash stimulation followed by 1 min of dark condition for 5 min, starting at 11 min after initiating infusion, to full scan time of 1 hour.

Data Analysis

Functional image calculations

Functional PET images were obtained as previously described (Giovacchini et al. 2002). For the first [1-^{11}C]AA injection, parametric images of the AA incorporation coefficient K* and

of cerebral blood volume V_b were derived by linearly fitting on a pixel-by-pixel basis the PET data with the following operational equation, which is based on an irreversible uptake model,

$$C_i(t) = V_b C_b(t) + K * \int_0^{60} C_p(s)ds + C_{CO_2}(t) \quad (1)$$

where $C_i(t)$ is brain radioactivity at time t, V_b is cerebral blood volume (mL blood/mL brain), $C_b(t)$ is whole blood activity (nCi/mL) at time t, $C_p(t)$ is the metabolite-corrected plasma input function, $C_{CO2}(t)$ is the predicted brain tissue concentration of [^{11}C]CO_2, and K* is the unidirectional incorporation coefficient of [1-^{11}C]AA (μL/min/mL).

For the second [1-^{11}C]AA scan, we modified equation (1) to take into account residual radioactivity from the first [1-^{11}C]AA scan,

$$C_i(t) = V_b^{(2)} C_b^{(2)}(t) + K*^{(2)} \int_0^{60} C_p{}^{(2)}(s)ds + C_{CO_2}{}^{(2)}(t) + K*^{(1)}\ d\int_0^{60} C_p{}^{(1)}(s)ds \quad (2)$$

where the correction term $K*^{(1)}\ d\int_0^{60} C_p{}^{(1)}(s)ds$ represents irreversibly bound uptake of tracer from the first scan and d equals the decay correction term between the two scans.

Image processing and statistical analysis

PET images of K*, V_b and rCBF were aligned to the structural MR image of each subject (Giovacchini et al. 2002). The images then were stereotactically normalized and smoothed with a 12 × 12 × 12 mm Gaussian filter using Statistical Parametric Mapping (SPM)-2 (http://www.fil.ion.ucl.ac.uk/spm/software/spm2/). rCBF and [1-^{11}C]AA data were ratio normalized to the global mean within SPM-2.

Statistical analyses tested for significant differences between visual stimulation at 2.9 or 7.8 Hz and the dark state (0 Hz), and between stimulation at 7.8 Hz and 2.9 Hz. Significant affected regions on SPM were identified from a human brain atlas (Talairach and Tournoux 1988), and are reported at $p \leq 0.001$ or $p \leq 0.01$ levels of significance. We also report absolute values of rCBF (mL/100 g/min) and of K* (μL/min/mL) in the significantly affected regions, percent differences as Δ% in these values, and cluster size (number of 2 mm × 2 mm × 2 mm voxels (8 mm^3)) of these regions. We did not correct the SPM-2 results for multiple comparisons, because we investigated an *a priori* hypothesis that rCBF and K* for AA would be altered by stimulation in widespread brain regions based on our prior measurements (Mentis et al. 1997), and because a prior study in unanesthetized rats indicated that percent changes in K* during visual stimulation would be about half the percent changes in rCBF (Wakabayashi et al. 1995).

Results

Regional cerebral blood flow

Figures 1A–1C illustrate regions on the surfaces of the cerebral hemispheres and in horizontal brain sections in which rCBF was significantly increased by flash stimulation ($p \leq 0.01$). Stimulation at 2.9 Hz or 7.8 Hz vs. 0 Hz (dark) increased rCBF in visual cortical and more anterior brain regions, and 7.8 Hz vs. 2.9 Hz increased rCBF in some of these regions as well.

Table 1 identifies Brodmann areas (BA) and their x-y-z coordinates in Talairach space, of the regions in which Z scores for differences during activation vs. dark exceeded 2.69 ($p \leq 0.01$) or 3.29 ($p \leq 0.001$). Stimulation at 7.8 Hz vs. 0 Hz significantly increased rCBF in the left-sided cuneus (BA 17 and 18), lingual gyrus (BA 18) and middle gyrus (BA 19) of the occipital

lobe, supramarginal gyrus of the parietal lobe (BA 40), fusiform gyrus of the temporal lobe (BA 37) and precentral gyrus of the frontal lobe (BA 6). Not shown are findings that stimulation at 7.8 Hz vs. 0 Hz significantly decreased rCBF in the anterior and posterior cingulate gyrus (BA 24 and 31), right insula (BA 13), superior temporal gyrus bilaterally (BA 21, 36 and 38), superior frontal gyrus bilaterally (BA 10 and 11), left premotor region (BA 4), right inferior frontal gyrus (BA 11 and 47), and postcentral gyrus bilaterally (BA 2).

Stimulation at 2.9 Hz vs. 0 Hz increased rCBF in the left-sided cuneus (BA 17) and lingual gyrus (BA 18) of the occipital lobe, precuneus (BA 31) and postcentral gyrus (BA 3) of the parietal lobe, and precentral gyrus of the frontal lobe (BA 4) (Table 1). Not shown are the findings that stimulation at 2.9 Hz vs. 0 Hz decreased rCBF in the right insula (BA 13), superior temporal gyrus bilaterally (BA 22, 42 and 48), right inferior temporal gyrus (BA 20), cerebellar vermis and right postcentral gyrus (BA 2 and 3), left superior parietal lobule (BA 7), right inferior and middle frontal gyrus (BA 45), left superior frontal gyrus (BA 9), and right supplementary motor area (BA 6). Stimulation at 7.8 Hz vs. 2.9 Hz increased rCBF in the cuneus (BA 17), inferior (BA 18) and middle (BA 19) gyrus of the occipital lobe, postcentral gyrus (BA 2) of the parietal lobe, and uncus (BA 38) of the limbic system (Table 1). Table 1 also summarizes cluster sizes of the positively affected regions, absolute values of rCBF and percent differences in these regions. Stimulation at 7.8 Hz vs. 0 Hz increased rCBF by a maximum of 22%, whereas stimulation at 2.9 Hz vs. 0 Hz increased rCBF by a maximum of 10%.

When the decreases in rCBF were considered in terms of absolute values (ml/100 g/min) without proportional SPM scaling, stimulation at 7.8 Hz vs. 0 Hz showed significant decreases of rCBF at $p < 0.05$ in the insula bilaterally (BA 13), the superior temporal gyrus bilaterally (BA 21, 36 and 38), the left superior frontal gyrus (BA 10), the postcentral gyrus bilaterally (BA 2), and both caudate nuclei. Stimulation at 2.9 Hz vs. 0 Hz showed decreases at $p < 0.01$ in the right insula (BA 13) and anterior cingulate gyrus (BA 31), and decreases at $p < 0.05$ in the superior temporal gyrus bilaterally (BA 22, 42 and 48), temporal gyri bilaterally (BA 20), in cerebellar vermis, postcentral gyri (BA 2 and 3), left superior parietal lobule (BA 7), inferior and middle frontal gyri bilaterally (BA 45), left superior frontal gyrus (BA 9) and right supplementary motor area (BA 6).

Arachidonic acid incorporation coefficients K*

Figures 2A–2C illustrate regions on the surface of the two hemispheres and in corresponding horizontal brain sections, in which K* for AA was significantly ($p \leq 0.01$) elevated as a function of flash frequency. Changes are evident in occipital and other visual areas.

Table 2 identifies regions in which stimulation at 2.9 Hz or 7.8 Hz flash vs. 0 Hz (dark) changed K* at the $p \leq 0.01$ ($Z \geq 2.69$) or $p \leq 0.001$ ($Z \geq 3.29$) level of significance, when considering only regions with cluster sizes greater than 40 pixels. Significant increments during 2.9 Hz or 7.8 Hz stimulation vs. 0 Hz ranged from 4.8% to 8.1% (Table 2). Affected areas roughly correspond to the areas in which rCBF was increased significantly (Table 1).

Significant elevations in K* at 7.8 Hz vs. 0 Hz were evident in the left cuneus (BA 19) and left superior gyrus (BA 11) of the occipital lobe, the right precuneus (BA 7)) and angular gyrus (BA 39) of the parietal lobe, right middle gyrus (BA 6 and 11), left paracentral lobule (BA 5), right superior gyrus (BA 11) of the frontal lobe, and right parahippocampal gyrus (BA 28) of the limbic lobe. Significant decreases at 7.8 Hz vs. 0 Hz (not shown) were seen in the right posterior cingulate gyrus (BA 31), right precuneus (BA 7), left inferior parietal lobule (BA 40), middle frontal gyrus bilaterally (BA 10 and 47), parahippocampal gyrus bilaterally (BA 28), left middle and right superior temporal gyri (BA 21 and 38), and right insula (BA 13).

At 2.9 Hz vs. 0 Hz, significant elevations in K* were found in the left cuneus of the occipital lobe (BA 17 and 19), postcentral gyrus bilaterally of the parietal lobe (BA 1), right middle gyrus of the temporal lobe (BA 21), medial gyrus of the frontal lobe (BA 6), claustrum, and left cerebellum. Significant decreases at 2.9 Hz vs. 0 Hz (not shown) were seen in the left precuneus (BA 30), left parahippocampal gyrus (BA 30), left fusiform gyrus (BA 19), anterior and posterior cingulate (BA 24 and 32, respectively), left middle occipital gyrus (BA 19), and left inferior frontal gyrus (BA 47), and cerebellum.

Comparison of Tables 2 and 1 indicates that the percent increments in absolute values of K*, 3.8–8.1%, were one-third to one-half percent increments in absolute values of rCBF.

When decreases in K* were considered in terms of absolute values (μL/min/mL), stimulation at 2.9 Hz vs. 0 Hz showed decreases at $p < 0.01$ in the left thalamus and in the left inferior frontal gyrus (BA 47) and at $p < 0.05$ in the left precuneus (BA 30), left parahippocampal gyrus (BA 30), left fusiform gyrus (BA 19), both inferior temporal gyri (BA 21), anterior and posterior cingulate (BA 24 and 32, respectively), and left middle occipital gyrus (BA 19).

Cerebral blood volume

There were many regions in which cerebral blood volume V_b was increased at $p \leq 0.01$ by 2.9 Hz or 7.8 Hz stimulation vs. the dark condition (0 Hz) (data not shown). Even at $p < 0.001$, V_b was elevated at 7.8 Hz vs. 0 Hz in the cerebellum, right frontal lobe (BA 10), lingual gyrus of the left occipital lobe (BA 17 and 18), and left superior temporal gyrus (BA 42), whereas it was elevated at 2.9 Hz vs. 0 Hz in the cerebellum, left pallidus, right thalamus, anterior and posterior cingulate gyrus (BA 32 and 23, respectively), right insula (BA 13) and right parahippocampal gyrus (BA 36), inferior and precentral gyrus of the right frontal lobe (BA 45 and 6, respectively), cuneus and lingual gyrus of the left occipital lobe (BA 17 and 18, respectively), inferior gyrus of the right temporal lobe (BA 20).

Discussion

This study shows that it is technically feasible to perform brain activation studies with PET and [1-^{11}C]AA, by presenting two stimuli, dark and 2.9 or 7.8 flash stimulation, in the same scan session. We used a linear irreversible model, which includes a correction for residual brain and plasma radioactivity from the prior [1-^{11}C]AA scan, to calculate K* for AA in the second [1-^{11}C]AA scan (Eq. 2). A single synthesis of [1-^{11}C]AA reduced cyclotron time and personnel needs, as well as the likelihood of technical problems.

Both K* for AA and rCBF were increased significantly in primary, association and related visual processing brain areas during 2.9 Hz and 7.8 Hz flash stimulation vs. the dark condition (0 Hz). Affected at both frequencies were regions in BA 17, 18 and 19, other areas in the two visual association streams in temporal and parietal regions (Ungerleider and Mishkin 1982), and certain frontal areas. Significant decrements, particularly in frontal areas not belonging to the two streams, were noted in both parameters. Cluster sizes of regions in which K* was altered were smaller than corresponding cluster sizes of regions in which rCBF was affected (Tables 1 and 2). This reflected in part the smaller magnitude of the K* changes, which would make their area of statistical significance smaller (centered towards the area of highest activation after smoothing).

The statistically significant rCBF changes during flash stimulation at 2.9 and 7.8 Hz vs. 0 Hz correspond in their location, magnitude and direction to changes reported in healthy subjects stimulated at comparable frequencies (Fox and Raichle 1984;Mentis et al. 1997). In these published studies, stimulation between 0 and 14 Hz produced biphasic increased and then decreasing rCBF changes in the striate cortex (BA 17) [peak 7–8 Hz] and left cingulate gyrus

(BA 24/32) [peak 4 Hz]. rCBF increased monotonically with frequency in lateral (inferior and medial occipital gyri and cuneus (BA 18 and 19) and inferior (lingual and fusiform gyri, BA 18 and 19) visual association areas, while decreasing monotonically in many anterior areas (frontal lobes, cingulate (BA 24, 32), superior temporal cortex). The left middle temporal area (BA 19/37) was activated at 1 Hz. It was suggested (Mentis et al. 1997) that the striate changes reflected lateral geniculate input, the middle temporal area activation at 1 Hz perception of apparent motion, and the posterior extrastriate rCBF monotonic increases a neural response to increasing luminance intensity and form and color complexity with increasing pattern-flash frequency.

Supporting our finding decreased rCBF and K* responses on SPM during stimulation at 2.9 Hz and 7.8 Hz, particularly in frontal areas, is that absolute values of these parameters also were reduced. In a more extensive study at flash frequencies between 0 and 14 Hz, significant reductions in absolute values of rCBF (ml/100g/min) also were found in many regions, including the medial and lateral frontal lobes and anterior cingulate cortex (Mentis et al. 1997). It was argued that these areas mediate higher order processing during executive functions, attention and language, and that their rCBF reductions represented cross-modal repression of their functional activity during the passive flash stimulus (Mentis et al. 1997). This explanation also could account for our reductions in K* for AA. Such cross-modal repression has been reported in the animal literature (Hernandez-Peon et al. 1956), in studies of evoked potentials in humans (Hackley et al. 1990), and in human imaging studies (Haxby et al. 1994;Kawashima et al. 1995;Mazziotta et al. 1982;Shulman et al. 1997).

Many of the statistically significant changes in K* for AA were in regions corresponding to those in which rCBF also was altered. Percent increments in K* in affected regions during stimulation at 2.9 or 7.8 Hz ranged from 3.8% to 8.1%, compared with 4.1% to 21% for significant rCBF increments. Smaller K* than rCBF increments were consistent with smaller K* that glucose metabolic increments in unanesthetized rats subjected to visual stimulation (Wakabayashi et al. 1995).

The increments in K* caused by visual stimulation likely arose by AA release from membrane phospholipid, mediated by any of a number of neuroreceptors coupled to the activation of $cPLA_2$ (see Introduction). Dopaminergic, glutamatergic, cholinergic and serotonergic neurotransmission can be involved in visual responses (Edagawa et al. 2000;Mentis et al. 2001;Yashiro et al. 2005;Zhao et al. 2001). However, glutamate is the main neurotransmitter of the brain visual system (Yashiro et al. 2005), and when acting at ionotropic NMDA receptors, glutamate allows Ca^{2+} into neurons to stimulate $cPLA_2$, release AA, and increase prostaglandin E_2 (PGE_2) formation (Basselin et al. 2006a;Pepicelli et al. 2002;Weichel et al. 1999). Thus, glutamatergic signaling *via* NMDA receptors likely was the major contributor to the significant changes in K* in this study.

rCBF is coupled to regional brain glucose metabolism (Reivich 1974), which is considered to reflect energy consumption largely by activation of pre-synaptic axon terminals (Sokoloff 1977;Sokoloff 1999). On the other hand, increments in K* represent the quantity of PLA_2-induced release of unesterified AA from synaptic membrane phospholipid and converted to eicosanoids such as PGE_2 (Basselin et al. 2006b;Jones et al. 1996;Rapoport 2003;Robinson et al. 1992). Thus, percent changes in rCBF and K* during activation need not be identical or exactly co-localized.

K* for AA is unaffected by changes in rCBF (Chang et al. 1997;DeGeorge et al. 1991;Rapoport 2003;Robinson et al. 1992), but is determined by brain metabolic demand (Basselin et al. 2006b;Jones et al. 1996;McArthur et al. 1999;Rapoport 2003). On the other hand, rCBF may be modified by PGE_2 and other vasoactive eicosanoids produced *via* cyclooxygenase-2 from

the AA released by PLA_2 activation. Thus, inhibiting cyclooxygenase-2 in rat brain with a nonsteroidal anti-inflammatory drug reduces rCBF increments during somatosensory stimulation (Li et al. 1995;Niwa et al. 2000).

In summary, we have established a two-condition paradigm in the same PET session to examine K* for AA and rCBF during sensory stimulation. We found that visual flash stimulation at 2.9 and 7.8 Hz produced significant changes in K* in areas in which significant changes in rCBF also were produced. The ability to image brain signal transduction involving AA should make the two-condition PET paradigm useful for examining regional effects of other sensory stimuli as well as of drug induced neuroreceptor activation (Basselin et al. 2006a;Basselin et al. 2006b;Bhattacharjee et al. 2005;Qu et al. 2003) in human subjects, under normal conditions and in diseases where neurotransmission *via* AA likely is disturbed (Hayakawa et al. 2001;Nariai et al. 1991).

In this regard, our studies in rat models of Parkinson disease (rats with a chronic unilateral lesion of the substantia nigra) and of Alzheimer disease (rats with a chronic unilateral lesion of the nucleus basalis) have demonstrated upregulated K* responses in brain regions ipsilateral to the lesion following administration of a dopaminergic D_2 receptor agonist or a muscarinic $M_{1,3,5}$ receptor agonist, respectively. Both D_2 and $M_{1,3,5}$ receptor subtypes can be coupled to $cPLA_2$ to release AA as a second messenger (Bhattacharjee et al. 2005;Felder et al. 1990;Vial and Piomelli 1995). Additionally, nicotine, given to rats at a dose equivalent to smoking one cigarette and saturating 85% of brain $\alpha_4\beta_2$ nicotinic receptors in humans (Brody et al. 2006), elevates K* for AA in widespread brain regions, including the nucleus accumbens (Nguyen et al. 2006). These animal studies suggest that PET can be used with our two-condition stimulation paradigm to image dopaminergic, muscarinic or nicotinic receptor-initiated AA signaling and concurrent changes in rCBF under normal or pathological human conditions, using receptor-directed drugs that have been reported to acutely change human rCBF or brain glucose metabolism (Furey et al. 2000;Grasby et al. 1993;Zubieta et al. 2005).

Supplementary Material

Refer to Web version on PubMed Central for supplementary material.

Acknowledgements

This work was supported by the intramural program of the National Institute on Aging. We thank Dr. Mark Mentis for his help in formulating this protocol.

References

Basselin M, Chang L, Bell JM, Rapoport SI. Chronic lithium chloride administration attenuates brain NMDA receptor-initiated signaling via arachidonic acid in unanesthetized rats. Neuropsychopharmacology 2006a;31:1659–1674. [PubMed: 16292331]

Basselin M, Villacreses NE, Langenbach R, Ma K, Bell JM, Rapoport SI. Resting and arecoline-stimulated brain metabolism and signaling involving arachidonic acid are altered in the cyclooxygenase-2 knockout mouse. J Neurochem 2006b;96:669–679. [PubMed: 16405503]

Bayon Y, Hernandez M, Alonso A, Nunez L, Garcia-Sancho J, Leslie C, Sanchez Crespo M, Nieto ML. Cytosolic phospholipase A_2 is coupled to muscarinic receptors in the human astrocytoma cell line 1321N1: characterization of the transducing mechanism. Biochem J 1997;323:281–287. [PubMed: 9173894]

Bhattacharjee AK, Chang L, Lee HJ, Bazinet RP, Seemann R, Rapoport SI. D_2 but not D_1 dopamine receptor stimulation augments brain signaling involving arachidonic acid in unanesthetized rats. Psychopharmacology (Berl) 2005:180. [PubMed: 15986187]

Brody AL, Mandelkern MA, London ED, Olmstead RE, Farahi J, Scheibal D, Jou J, Allen V, Tiongson E, Chefer SI, Koren AO, Mukhin AG. Cigarette smoking saturates brain alpha 4 beta 2 nicotinic acetylcholine receptors. Arch Gen Psychiatry 2006;63:907–915. [PubMed: 16894067]

Chang MCJ, Arai T, Freed LM, Wakabayashi S, Channing MA, Dunn BB, Der MG, Bell JM, Sasaki T, Herscovitch P, Eckelman WC, Rapoport SI. Brain incorporation of [1-^{11}C]-arachidonate in normocapnic and hypercapnic monkeys, measured with positron emission tomography. Brain Res 1997;755:74–83. [PubMed: 9163542]

Channing MA, Simpson N. Radiosynthesis of 1-[11C]polyhomoallylic fatty acids. J Labeled Compounds Radiopharmacol 1993;33:541–546.

Clark JD, Schievella AR, Nalefski EA, Lin LL. Cytosolic phospholipase A2. J Lipid Mediat Cell Signal 1995;12:83–117. [PubMed: 8777586]

Cooper, JR.; Bloom, FE.; Roth, RH. The Biochemical Basis of Neuropharmacology. Oxford: Oxford University Press; 2003.

DeGeorge JJ, Nariai T, Yamazaki S, Williams WM, Rapoport SI. Arecoline-stimulated brain incorporation of intravenously administered fatty acids in unanesthetized rats. J Neurochem 1991;56:352–355. [PubMed: 1824784]

Edagawa Y, Saito H, Abe K. The serotonin 5-HT2 receptor-phospholipase C system inhibits the induction of long-term potentiation in the rat visual cortex. Eur J Neurosci 2000;12:1391–1396. [PubMed: 10762367]

Esposito G, Giovacchini G, Der MG, Vuong BK, Channing MA, Lerner A, Hallett M, Battacharjee AK, Herscovitch P, Eckelman WC, Rapoport SI, Carson RE. [11C]Arachidonic acid PET activation experiments in human subjects: A feasibility study using visual stimulation. J Cereb Blood Flow Metab 2003;23 (Suppl 1):711.

Felder CC, Dieter P, Kinsella J, Tamura K, Kanterman RY, Axelrod J. A transfected m5 muscarinic acetylcholine receptor stimulates phospholipase A_2 by inducing both calcium influx and activation of protein kinase C. J Pharmacol Exp Ther 1990;255:1140–1147. [PubMed: 2124620]

Fox PT, Mintun MA, Raichle ME, Herscovitch P. A noninvasive approach to quantitative functional brain mapping with H_2O15 and positron emission tomography. J Cereb Blood Flow Metabol 1984;4:329–333.

Fox PT, Raichle ME. Stimulus rate dependence of regional cerebral blood flow in human striate cortex, demonstrated by positron emission tomography. J Neurophysiol 1984;51:1109–1120. [PubMed: 6610024]

Furey ML, Pietrini P, Alexander GE, Mentis MJ, Szczepanik J, Shetty U, Greig NH, Holloway HW, Schapiro MB, Freo U. Time course of pharmacodynamic and pharmacokinetic effects of physostigmine assessed by functional brain imaging in humans. Pharmacol Biochem Behav 2000;66:475–481. [PubMed: 10899358]

Giovacchini G, Chang MC, Channing MA, Toczek M, Mason A, Bokde AL, Connolly C, Vuong BK, Ma Y, Der MG, Doudet DJ, Herscovitch P, Eckelman WC, Rapoport SI, Carson RE. Brain incorporation of [11C]arachidonic acid in young healthy humans measured with positron emission tomography. J Cereb Blood Flow Metab 2002;22:1453–1462. [PubMed: 12468890]

Giovacchini G, Lerner A, Toczek MT, Fraser C, Ma K, DeMar JC, Herscovitch P, Eckelman WC, Rapoport SI, Carson RE. Brain incorporation of 11C-arachidonic acid, blood volume, and blood flow in healthy aging: a study with partial-volume correction. J Nucl Med 2004;45:1471–1479. [PubMed: 15347713]

Grange E, Rabin O, Bell J, Chang MC. Manoalide, a phospholipase A_2 inhibitor, inhibits arachidonate incorporation and turnover in brain phospholipids of the awake rat. Neurochem Res 1998;23:1251–1257. [PubMed: 9804280]

Grasby PM, Friston KJ, Bench CJ, Cowen PJ, Frith CD, Liddle PF, Frackowiak RS, Dolan RJ. The effect of the dopamine agonist, apomorphine, on regional cerebral blood flow in normal volunteers. Psychol Med 1993;23:605–612. [PubMed: 7901864]

Hackley SA, Woldorff M, Hillyard SA. Cross-modal selective attention effects on retinal, myogenic, brainstem, and cerebral evoked potentials. Psychophysiology 1990;27:195–208. [PubMed: 2247550]

Haxby JV, Horwitz B, Ungerleider LG, Maisog JM, Pietrini P, Grady CL. The functional organization of human extrastriate cortex: a PET-rCBF study of selective attention to faces and locations. J Neurosci 1994;14:6336–6353. [PubMed: 7965040]

Hayakawa T, Chang MC, Rapoport SI, Appel NM. Selective dopamine receptor stimulation differentially affects [3H]arachidonic acid incorporation, a surrogate marker for phospholipase A2-mediated neurotransmitter signal transduction, in a rodent model of Parkinson's disease. J Pharmacol Exp Ther 2001;296:1074–1084. [PubMed: 11181943]

Hernandez-Peon R, Scherrer H, Jouvet M. Modification of electric activity in cochlear nucleus during attention in unanesthetized cats. Science 1956;123:331–332. [PubMed: 13298689]

Herscovitch P, Markham J, Raichle ME. Brain blood flow measured with intravenous H2(15)O. I. Theory and error analysis. J Nucl Med 1983;24:782–789. [PubMed: 6604139]

Jones CR, Arai T, Bell JM, Rapoport SI. Preferential in vivo incorporation of [3H]arachidonic acid from blood in rat brain synaptosomal fractions before and after cholinergic stimulation. J Neurochem 1996;67:822–829. [PubMed: 8764612]

Kawashima R, O'Sullivan BT, Roland PE. Positron emission tomography studies of cross-modality inhibition in selective attentional tasks: closing the "mind's eye". Proc Natl Acad Sci (USA) 1995;92:5969–5972. [PubMed: 7597062]

Li DY, Varma DR, Chemtob S. Up-regulation of brain PGE2 and PGF2 alpha receptors and receptor-coupled second messengers by cyclooxygenase inhibition in newborn pigs. J Pharmacol Exp Ther 1995;272:15–19. [PubMed: 7815327]

Mazziotta JC, Phelps ME, Carson RE, Kuhl DE. Tomographic mapping of human cerebral metabolism: Auditory stimulation. Neurol 1982;32:921–937.

McArthur MJ, Atshaves BP, Frolov A, Foxworth WD, Kier AB, Schroeder F. Cellular uptake and intracellular trafficking of long chain fatty acids. J Lipid Res 1999;40:1371–1383. [PubMed: 10428973]

Mentis MJ, Alexander GE, Grady CL, Horwitz B, Krasuski J, Pietrini P, Strassburger T, Hampel H, Schapiro MB, Rapoport SI. Frequency variation of a pattern-flash visual stimulus during PET differentially activates brain from striate through frontal cortex. Neuroimage 1997;5:116–128. [PubMed: 9345542]

Mentis MJ, Alexander GE, Krasuski J, Pietrini P, Furey ML, Schapiro MB, Rapoport SI. Increasing required neural response to expose abnormal brain function in mild versus moderate or severe Alzheimer's disease: PET study using parametric visual stimulation. Am J Psychiatry 1998;155:785–794. [PubMed: 9619151]

Mentis MJ, Horwitz B, Grady CL, Alexander GE, VanMeter JW, Maisog JM, Pietrini P, Schapiro MB, Rapoport SI. Visual cortical dysfunction in Alzheimer's disease evaluated with a temporally graded "stress test" during PET. Am J Psychiatry 1996;153:32–40. [PubMed: 8540589]

Mentis MJ, Sunderland T, Lai J, Connolly C, Krasuski J, Levine B, Friz J, Sobti S, Schapiro M, Rapoport SI. Muscarinic versus nicotinic modulation of a visual task. A PET study using drug probes. Neuropsychopharmacology 2001;25:555–564. [PubMed: 11557169]

Nariai T, DeGeorge JJ, Lamour Y, Rapoport SI. In vivo brain incorporation of [1-^{14}C]arachidonate in awake rats, with or without cholinergic stimulation, following unilateral lesioning of nucleus basalis magnocellularis. Brain Res 1991;559:1–9. [PubMed: 1723641]

Nguyen, HN.; Villacreses, NE.; Chang, L.; Rapoport, SI. Imaging nicotine-induced brain signal transduction via arachidonic acid in awake rats. Soc Neurosci Abstr; Atlanta, GA: 2006. p. 416-419.

Niwa K, Araki E, Morham SG, Ross ME, Iadecola C. Cyclooxygenase-2 contributes to functional hyperemia in whisker-barrel cortex. J Neurosci 2000;20:763–770. [PubMed: 10632605]

Pepicelli O, Fedele E, Bonanno G, Raiteri M, Ajmone-Cat MA, Greco A, Levi G, Minghetti L. In vivo activation of N-methyl-D-aspartate receptors in the rat hippocampus increases prostaglandin E(2) extracellular levels and triggers lipid peroxidation through cyclooxygenase-mediated mechanisms. J Neurochem 2002;81:1028–1034. [PubMed: 12065615]

Qu Y, Chang L, Klaff J, Balbo A, Rapoport SI. Imaging brain phospholipase A_2 activation in awake rat in response to 5-$HT_{2A/2C}$ agonist (+/−)-2,5-dimethoxy-4-iodophenyl-2-aminopropane (DOI). Neuropsychopharmacology 2003;28:244–252. [PubMed: 12589377]

Rakshi JS, Pavese N, Uema T, Ito K, Morrish PK, Bailey DL, Brooks DJ. A comparison of the progression of early Parkinson's disease in patients started on ropinirole or L-dopa: an (18)F-dopa PET study. J Neural Transm 2002;109:1433–1443. [PubMed: 12486484]

Rapoport SI. In vivo approaches to quantifying and imaging brain arachidonic and docosahexaenoic acid metabolism. J Pediatr 2003;143:S26–S34. [PubMed: 14597911]

Rapoport SI, Bosetti F. Do lithium and anticonvulsants target the brain arachidonic acid cascade in bipolar disorder? Arch Gen Psychiatry 2002;59:592–596. [PubMed: 12090811]

Reivich M. Blood flow metabolism couple in brain. Res Publ Assoc Res Nerv Ment Dis 1974;53:125–140. [PubMed: 4216058]

Robinson PJ, Noronha J, DeGeorge JJ, Freed LM, Nariai T, Rapoport SI. A quantitative method for measuring regional in vivo fatty-acid incorporation into and turnover within brain phospholipids: Review and critical analysis. Brain Res Rev 1992;17:187–214. [PubMed: 1467810]

Shulman GL, Corbetta M, Buckner RL, Raichle ME, Fiez JA, Miezin FM, Petersen SE. Top-down modulation of early sensory cortex. Cereb Cortex 1997;7:193–206. [PubMed: 9143441]

Sokoloff L. Relation between physiological function and energy metabolism in the central nervous system. J Neurochem 1977;29:13–26. [PubMed: 407330]

Sokoloff L. Energetics of functional activation in neural tissues. Neurochem Res 1999;24:321–329. [PubMed: 9972882]

Solanto MV. Dopamine dysfunction in AD/HD: integrating clinical and basic neuroscience research. Behav Brain Res 2002;130:65–71. [PubMed: 11864719]

Stout BD, Clarke WP, Berg KA. Rapid desensitization of the serotonin(2C) receptor system: effector pathway and agonist dependence. J Pharmacol Exp Ther 2002;302:957–962. [PubMed: 12183652]

Talairach, J.; Tournoux, P. Co-planar stereotaxic atlas of the human brain. New York; Thieme Medical Publishers, Inc: 1988.

Ungerleider, LG.; Mishkin, M. Two cortical visual systems. In: Ingle, DJ.; Goodale, MA.; Mansfield, RJW., editors. Analysis of Visual Behavior. Cambridge: MIT Press; 1982. p. 549-586.

Vial D, Piomelli D. Dopamine D2 receptors potentiate arachidonate release via activation of cytosolic, arachidonate-specific phospholipase A2. J Neurochem 1995;64:2765–2772. [PubMed: 7760057]

Wakabayashi S, Freed LM, Chang M, Rapoport SI. In vivo imaging of brain incorporation of fatty acids and of 2-deoxy-D-glucose demonstrates functional and structural neuroplastic effects of chronic unilateral visual deprivation in rats. Brain Res 1995;679:110–122. [PubMed: 7648253]

Weichel O, Hilgert M, Chatterjee SS, Lehr M, Klein J. Bilobalide, a constituent of Ginkgo biloba, inhibits NMDA-induced phospholipase A2 activation and phospholipid breakdown in rat hippocampus. Naunyn Schmiedebergs Arch Pharmacol 1999;360:609–615. [PubMed: 10619176]

Yashiro K, Corlew R, Philpot BD. Visual deprivation modifies both presynaptic glutamate release and the composition of perisynaptic/extrasynaptic NMDA receptors in adult visual cortex. J Neurosci 2005;25:11684–11692. [PubMed: 16354927]

Zhao Y, Kerscher N, Eysel U, Funke K. Changes of contrast gain in cat dorsal lateral geniculate nucleus by dopamine receptor agonists. Neuroreport 2001;12:2939–2945. [PubMed: 11588607]

Zubieta JK, Heitzeg MM, Xu Y, Koeppe RA, Ni L, Guthrie S, Domino EF. Regional cerebral blood flow responses to smoking in tobacco smokers after overnight abstinence. Am J Psychiatry 2005;162:567–577. [PubMed: 15741475]

Abbreviations

AA
: arachidonic acid

BA
: Brodmann area

LED
: light emitting diode

MRI
magnetic resonance imaging

NMDA
N-methyl-D-aspartic acid

PET
positron emission tomography

PGE_2
prostaglandin E_2

PLA_2
phospholipase A_2

$cPLA_2$
cytosolic PLA_2

SPM
statistical parametric mapping

rCBF
regional cerebral blood flow

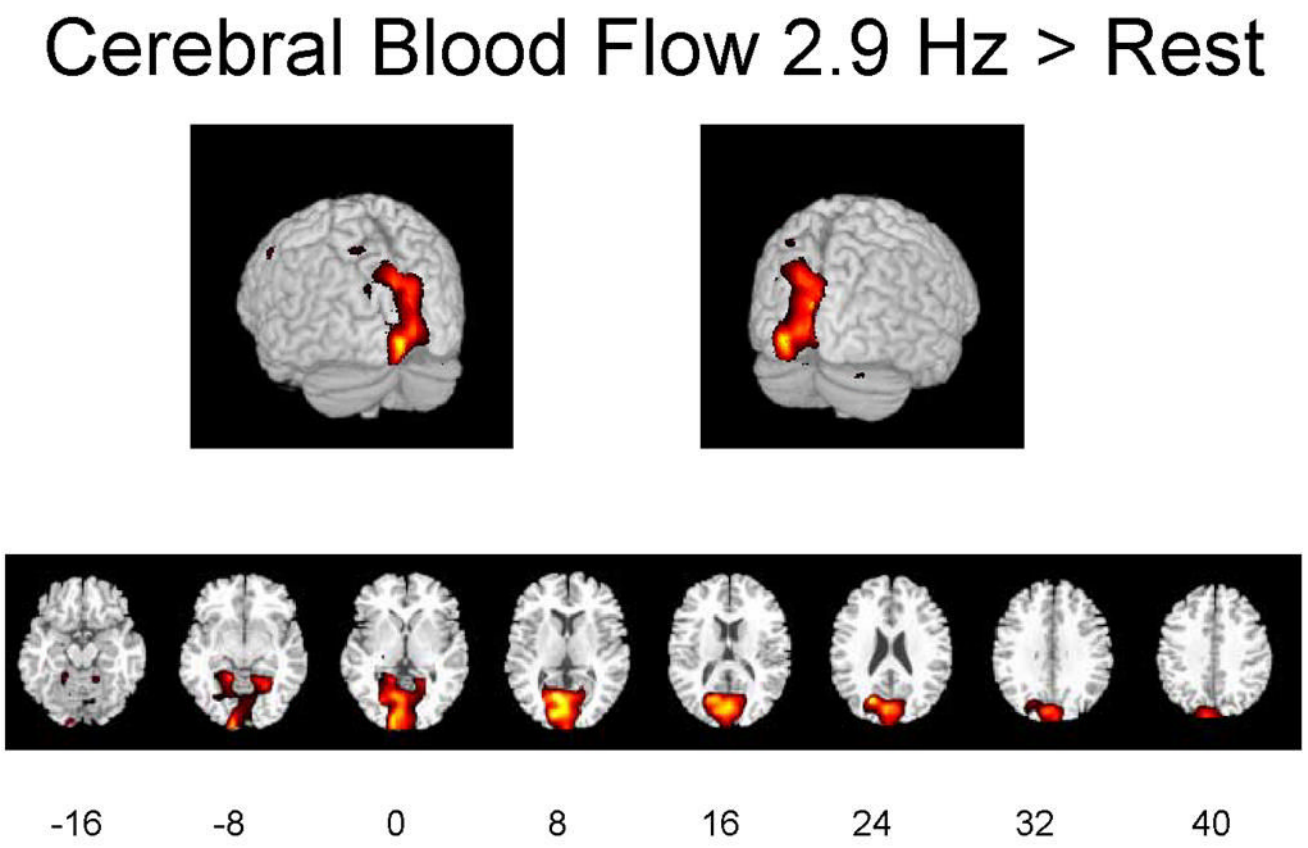

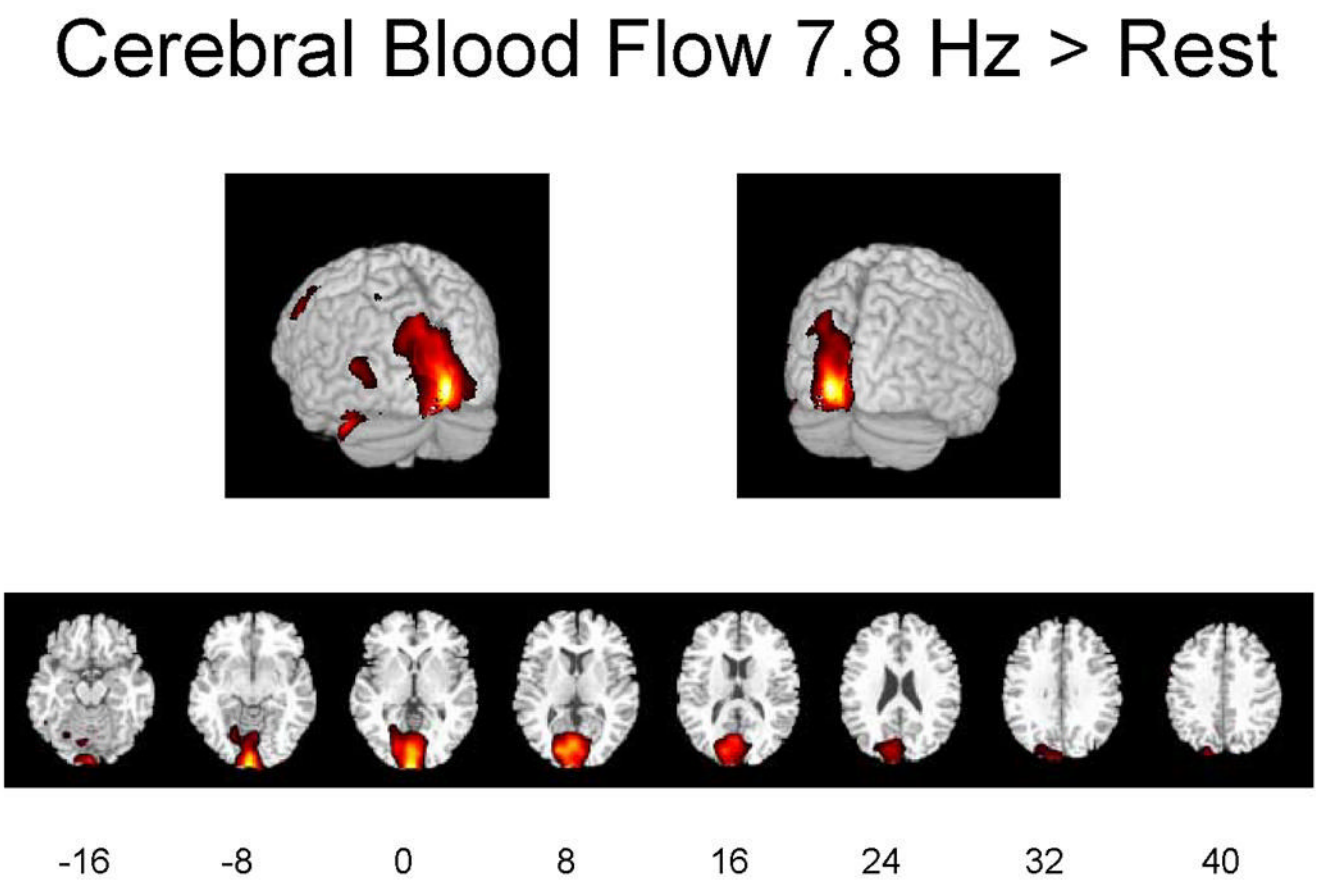

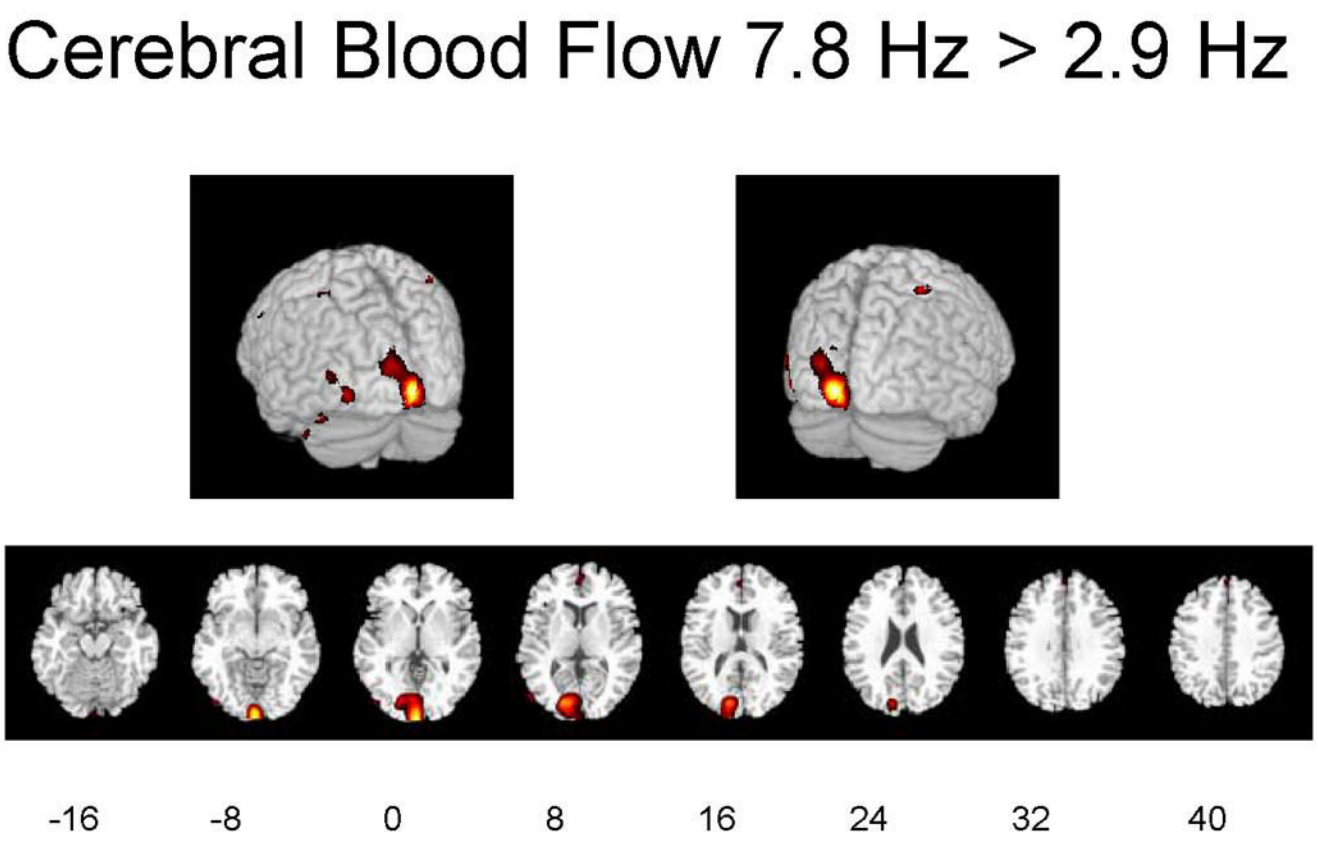

Figures 1A-1C. Hemispheric and horizontal renderings from MRI template of significant increases of rCBF between 2.9 Hz and 0 Hz (dark condition), 7.8 Hz and 0 Hz, and 7.8 Hz and 2.9 Hz flash stimulation

Significant differences at $p \leq 0.01$ are displayed in red. Eight different slices are displayed from the −16 mm level to the +40 mm level with regard to the anterior-posterior commissure line in Talairach space are shown (Talairach and Tournoux 1988).

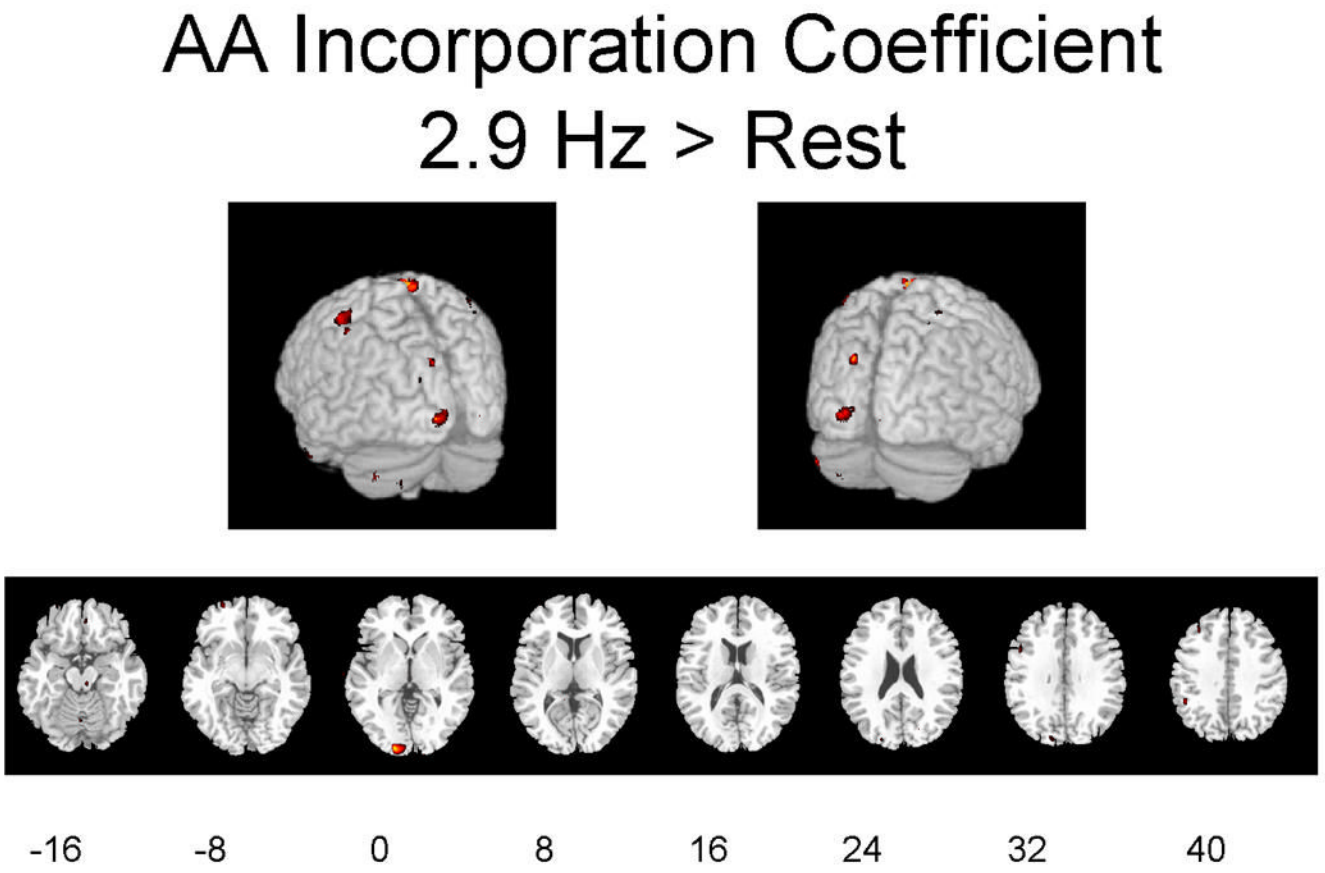

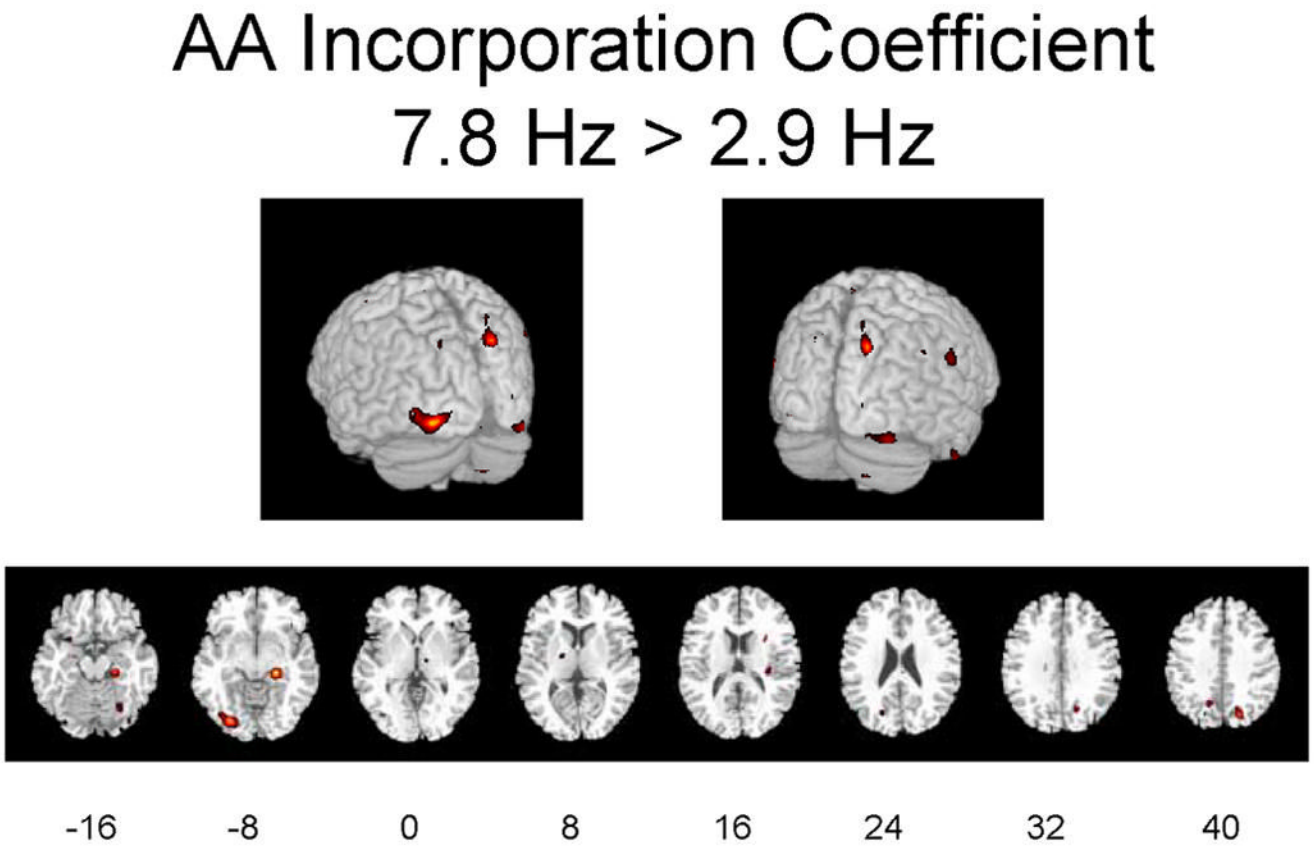

Figures 2A-2C. Hemispheric and horizontal renderings from MRI template of significant increases of K* for AA between 2.9 Hz and 0 Hz (dark condition), 7.8 Hz and 0 Hz, and 7.8 Hz and 2.9 Hz flash stimulation

Significant differences at $p \leq 0.01$ are displayed in red. Eight different slices are displayed from the −16 mm level to the +40 mm level in Talairach space are shown (Talairach and Tournoux 1988).

Table 1

Cerebral Blood Flow

Statistically significant increments in rCBF, at $p \leq 0.01$ (Z = 2.69) or $p \leq 0.001$ (Z = 3.29), between visual flash stimulation at 2.9 Hz or 7.8 Hz and dark (rest) condition (0 Hz), and between 7.8 Hz and 2.9 Hz stimulation conditions. X,Y and Z coordinates given in Talairach space (Talairach and Tournoux 1988). Cluster size given in voxels (8 mm^3). BA = Brodmann Area.

Visual Stimulation 7.8 Hz - Rest

Region		Side	BA	X	Y	Z	Z Score	Cluster Size (vox)	rCBF activ1	rCBF dark1	Δ%[2]
Frontal	Precentral Gyrus	L	6	60	0	42	3.5**	398.0	67.7	55.6	21.7
Occipital	Cuneus	L	17	18	−84	6	5.08**		114.6	94.4	21.3
Occipital	Cuneus	L	18	2	−104	0	5.7**	11564.0	74.9	64.1	16.9
Occipital	Lingual Gyrus	L	18	2	−82	4	5.1**		67.1	63.8	5.1
Occipital	Middle Gyrus	L	19	58	−74	12	3.75**	513.0	57.6	54.2	6.2
Parietal	Supramarginal Gyr	L	40	56	−58	−30	4.09**	540.0	54.7	51.5	6.1
Temporal	Fusiform Gyrus	L	37	48	−52	−12	3.38**		62.6	60.3	3.8

Visual Stimulation 2.9 Hz - Rest

Region		Side	BA	X	Y	Z	Z Score	Cluster Size (vox)	rCBF activ[1]	rCBF dark[1]	Δ%[2]
Frontal	Precentral Gyrus	L	4	54	−4	44	3.77**	408.0	96.7	87.7	10.3
Occipital	Cuneus	L	17	12	−86	8	6.06**		77.2	72.4	6.7
Occipital	Lingual Gyrus	L	18	8	−68	6	6.4**	16729.0	86.7	78.8	10.1
Parietal	Postcentral Gyrus	L	3	60	−14	48	3.12*		75.5	72.7	4.0
Parietal	Precuneus	L	31	20	−72	22	6.19**		58.0	55.0	5.5
		L		32	−40	−50	3.31**	110.0	58.4	56.1	4.1

Activation at 7.8 Hz > Activation at 2.9 Hz

Region		Side	BA	X	Y	Z	Z Score	Cluster Size (vox)	Δ%[2] 2.9 Hz	Δ%[2]7.8 Hz
Limbic	Uncus	R	38	−20	10	−28	3.21*	136.0	7.1	21.6
Occipital	Cuneus	L	17	16	−84	6	3.76**		8.4	17.2
Occipital	Cuneus	R	17	0	−100		4.43**	2443.0	0.4	7.5
Occipital	Inferior Gyrus	L	18	44	−88	−4	3.13*		−3.7	2.6
Occipital	Middle Gyrus	L	19	56	−76	12	3.26*	254.0	−4.1	4.3

[1] ml/100g/min

[2] Percent difference caused by activation

BA = Brodmann area; vox = voxels

Significant difference between means,

* $p < 0.01$,

*** $p < 0.001$

Table 2

Arachidonic Acid Incorporation Coefficient K*

Statistically significant differences in K^* for AA, at $p \leq 0.01$ ($Z = 2.69$) or $p \leq 0.001$ ($Z = 3.29$), between visual stimulation condition at 2.9 Hz or 7.8 Hz and dark (rest) condition (0 Hz), and between 7.8 Hz and 2.9 Hz stimulation conditions. X,Y and Z coordinates given in Talairach space (Talairach and Tournoux 1988). Cluster size given in voxels (8 mm^3). BA = Brodmann Area

Visual Stimulation 7.8 Hz - Rest

Region		Side	BA	X	Y	Z	Z Score	Cluster Size (vox)	K activ *1	K dark *1	Δ%2
Frontal	Middle Gyrus	R	11	−34	36	−14	3.68**	921.0	7.0	6.5	7.5
Frontal	Paracentral Lobule	L	5	22	−42	44	3.91**	45.0	7.2	6.8	5.3
Occipital	Cuneus	L	19	14	−96	28	3.46**	69.0	6.8	6.5	5.0
Parietal	Angular Gyrus	R	39	−58	−60	38	3.59**	52.0	5.5	5.4	2.9
Parietal	Precuneus	R	7	−22	−76	40	3.52**	97.0	5.3	5.1	3.7

Visual Stimulation 2.9 Hz - Rest

Region		Side	BA	X	Y	Z	Z Score	Cluster Size (vox)	K* activ1	K* dark1	Δ%2
Cerebellum		L		18	−74	−30	3.41**	115.0	5.9	5.7	3.9
Occipital	Cuneus	L	17	14	−98	0	3.46**	166.0	5.3	5.1	3.6
Parietal	Postcentral	L	1	46	−30	58	3.13*	226.0	7.1	7.0	2.3
Parietal	Postcentral	R	1	−2	−36	78	3.4**	214.0	7.2	6.6	8.9
Subcortical	Claustrum	L		46	−80	−42	3.13*	76.0	5.8	5.6	3.9
Temporal	Middle Gyrus	R	21	−42	2	−32	3.46**	64.0	7.1	6.9	4.1

Activation at 7.8 Hz > Activation at 2.9 Hz

Region		Side	BA	X	Y	Z	Z Score	Cluster Size (vox)	Δ%2 2.9 Hz	Δ%2 7.8 Hz
Limbic	Parahippocampal	R	35	−26	−26	−12	4.02**	210.0	−6.1	3.0
Occipital	Middle Gyrus	L	18	28	−80	−10	3.72**	306.0	−3.2	3.2
Parietal	Precuneus	R	7	−22	−74	40	3.4**	177.0	−2.6	4.0

[1] μL/min/mL

[2] Δ%, per cent difference

BA = Brodmann area; vox = voxels

Significant difference between means,

* $p < 0.01$,

*** $p < 0.001$